High-Temperature Superconducting Phases in Cerium Superhydride with a T_c up to 115 K below a Pressure of 1 Megabar

Wuhao Chen,[1] Dmitrii V. Semenok,[2] Xiaoli Huang,[1,*] Haiyun Shu,[4] Xin Li,[1] Defang Duan,[1] Tian Cui,[3,1,†] and Artem R. Oganov[2]

[1]State Key Laboratory of Superhard Materials, College of Physics, Jilin University, Changchun 130012, China
[2]Skolkovo Institute of Science and Technology, Skolkovo Innovation Center, Bolshoy Boulevard 30, bldg. 1 Moscow, Russia 121205
[3]School of Physical Science and Technology, Ningbo University, Ningbo 315211, China
[4]Center for High Pressure Science and Technology Advanced Research, Shanghai 201203, China

(Received 9 January 2021; accepted 30 July 2021; published 9 September 2021)

The discoveries of high-temperature superconductivity in H_3S and LaH_{10} have excited the search for superconductivity in compressed hydrides, finally leading to the first discovery of a room-temperature superconductor in a carbonaceous sulfur hydride. In contrast to rapidly expanding theoretical studies, high-pressure experiments on hydride superconductors are expensive and technically challenging. Here, we experimentally discovered superconductivity in two new phases, $Fm\bar{3}m$-CeH_{10} (SC-I phase) and $P6_3/mmc$-CeH_9 (SC-II phase) at pressures that are much lower (<100 GPa) than those needed to stabilize other polyhydride superconductors. Superconductivity was evidenced by a sharp drop of the electrical resistance to zero and decreased critical temperature in deuterated samples and in external magnetic field. SC-I has $T_c = 115$ K at 95 GPa, showing an expected decrease in further compression due to the decrease of the electron-phonon coupling (EPC) coefficient λ (from 2.0 at 100 GPa to 0.8 at 200 GPa). SC-II has $T_c = 57$ K at 88 GPa, rapidly increasing to a maximum $T_c \sim 100$ K at 130 GPa, and then decreasing in further compression. According to the theoretical calculation, this is due to a maximum of λ at the phase transition from $P6_3/mmc$-CeH_9 into a symmetry-broken modification $C2/c$-CeH_9. The pressure-temperature conditions of synthesis affect the actual hydrogen content and the actual value of T_c. Anomalously low pressures of stability of cerium superhydrides make them appealing for studies of superhydrides and for designing new superhydrides with stability at even lower pressures.

DOI: 10.1103/PhysRevLett.127.117001

The search for high-temperature superconductivity is one of the most attractive tasks of condensed matter physics and materials science [1–3]. An appealing idea dating back to the early 1960s was that metallic hydrogen should be a high-temperature superconductor [4–7]. Because of the small mass of hydrogen, phonon frequencies in metallic hydrogen would be very high, of the order of several thousand kelvins [8], while covalent bonding will lead to strong electron-phonon coupling. However, the transition of hydrogen from molecular insulating phase into the metallic state requires extremely high pressures [6,9,10]. For this reason, in recent years, researchers have started to introduce the superconducting state by adding other elements to hydrogen [11–16], with the idea that chemical precompression of hydrogen [17] results in a strong reduction of the metallization pressure while maintaining high T_c.

Several hydrogen-rich superconductors have been synthesized in succession [18–24]. In 2014, an unusual high-pressure compound H_3S with superconductivity at 191–204 K had been predicted [25] and later experimentally obtained [21,26], ushering in a new era in studies of superconductivity. In 2019, this record of high-temperature superconductivity was broken, with LaH_{10} experimentally proven to have nearly room-temperature superconductivity with T_c of 250–260 K [18,19]. The high critical temperature results from the strong interaction of wide-band electrons with high-frequency phonons (optical modes caused by the presence of light hydrogen ions) [27,28]. The current highest T_c of 288 K at ~267 GPa was reported recently in the C–S–H system [29], which indeed set a major milestone in the history of superconductivity by reaching room-temperature superconductivity. Very recently, Snider *et al.* reported a yttrium superhydride that exhibits superconductivity with a T_c of 262 K at 182 GPa, by using a special synthesis method [30]. Until now, the experimentally obtained high-temperature superconducting hydrides only exist above megabar pressure. Now the challenge is to find compounds exhibiting comparable superconducting properties at or close to ambient pressures, especially in experiment. Though some appealing ternary hydrides have been predicted [31–35], binary hydrides are easier to synthesize and characterize, and their knowledge helps to focus on the most promising ternary and more complex systems.

Cerium polyhydride hcp-CeH_9 was synthesized at around 90 GPa with each Ce atom enclosed in an H_{29}

cage of the atomic hydrogen sublattice [36,37]. For the related compounds, the calculated T_c reaches only 56 K [38] and 63–75 K [37] at 100 GPa, respectively. Accompanying the subsequent prediction of two cubic phases ($Fm\bar{3}m$-CeH_{10} and $F\bar{4}3m$-CeH_9), T_c is boosted to over 140 K at 94 GPa [39]. In this study, we experimentally discovered superconductivity both in CeH_9 and the newly synthesized CeH_{10}. We also discussed the quite different behavior of these superconductors in the context of both experiment and theory.

In previous work [36,37], two synthetic paths to $P6_3/mmc$-CeH_9 were confirmed: both cold compression and high-temperature annealing of Ce in hydrogen (H_2). Here, we used the ammonia borane (NH_3BH_3, or AB for shorthand) as the source of hydrogen released on heating due to decomposition reaction $NH_3BH_3 \rightarrow 3H_2 + c$-BN [40–42]. This approach has been successfully used in several recent studies [19,20,22,43,44]. Pressure was determined using the Raman shift of diamond [45], calibrated by Akahama [46].

We performed six experimental runs (cells H1–H6) to investigate superconductivity in the Ce—H system at high pressures. The scheme of assembly used for the electrical measurements is shown in the inset of Fig. 1(b). The details of experimental methods and the parameters of cells H1–H6 are presented in Supplemental Material [47]. The Ce sample was placed inside the DAC with four deposited Mo electrodes [66] and photographed after heating [Fig. 1(a)]. The heated part expanded due to the increased hydrogen content, and the pressure decreased about 8 GPa in both cells H1 and H4. The Raman vibron of H_2 was detected, indicating a local excess of hydrogen necessary to form cerium polyhydrides [Supplemental Material, Figs. S6 and S19]. However, no extra Raman signal except the ones that come from the background were detected [Fig. S20]. The R-T dependences in cooling and warming cycles are pretty close except in cell H1 because of the too fast temperature changing rate. This inconsistency is mainly because of the temperature hysteresis between the sample and thermometer. In cell H1, pressure decreased from 95 to 88 GPa after laser heating, and the electrical resistance dropped sharply to zero from 49 K (Fig. S7). However, we observed the step-like transition curves in cells H2 and H3 heated at similar pressures (90–100 GPa), and the onset of transition temperature increased a lot [Fig. 1(b)]. We tentatively proposed that the two prominent T_{c1} and T_{c2} come from disparate phases. Upon further compression of cell H2, the superconducting transition width decreases, reflecting different pressure dependences of these critical temperatures. Noteworthy, the transition temperature is reversible during decompression (Fig. S12). To increase the T_c, we heated cell H3 several times at 100 GPa and reheated cells H4 and H5 at 100 and 136 GPa, respectively. Then, steplike transitions were also obtained, whereas cell H3 broke (Fig. S16).

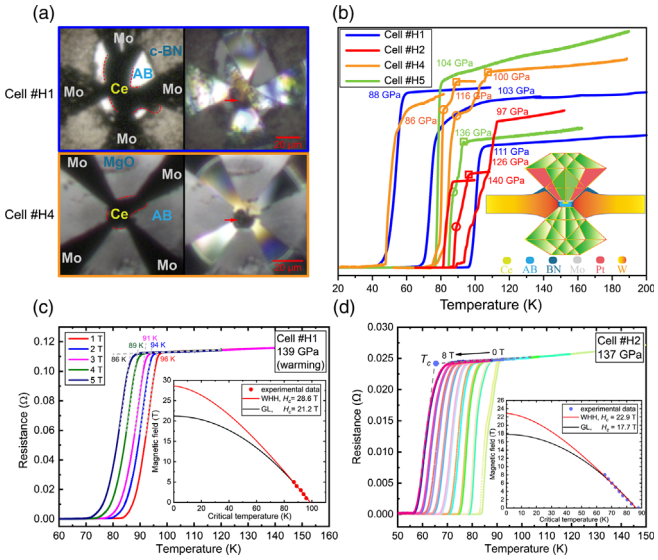

FIG. 1. Superconducting transitions determined by the electrical resistivity measurements in typical cells. (a) Pressurized Ce/AB sample and four electrodes on the insulated gasket in cells H1 and H4 with bottom (left) and double-side illumination (right). The edge of cerium is marked with red dotted lines and the red arrows point to the parts with apparent changes. (b) Temperature dependence of the electrical resistance at the superconducting transitions (the warming cycle) in DACs H1-5 at selected pressures. Squares and circles indicate the apparent turning points. The scheme of the experimental assembly is shown in the inset. (c),(d) R-T dependence in a magnetic field of 1–5 T at 139 GPa (cell H1, warming cycle) and 0–8 T at 137 GPa (cell H2). Dashed lines are linear fittings of the normal and transition states, and T_c is defined at their intersection. The upper critical magnetic fields estimated using the Werthamer-Helfand-Hohenberg (WHH) [67] and Ginzburg-Landau (GL) [68] theories are shown in the inset. Warm and cool colors represent warming and cooling cycles, respectively in (d).

We compared cells H1 and H2 in the external magnetic field at around 140 GPa [Figs. 1(c) and 1(d)]. In cell H1, T_c decreases from 96 K (1 T) to 86 K (5 T) [Fig. 1(c)], yielding the slope of the critical field $dH_c/dT = -0.4$ T/K. The applied magnetic fields are insufficient to directly determine the upper critical magnetic field (H_{c2}) at 0 K. Therefore, we extrapolated $H_{c2}(0) \sim 21.2$ and 28.6 T using Ginzburg-Landau (GL $1 - t^2$ model) [68,69] and Werthamer-Helfand-Hohenberg (WHH) [67] formulas, respectively. The applied magnetic field of 8 T to cell H2 lowers T_c by 23 K. Extrapolations based on GL and WHH expressions yield $H_{c2}(0) \sim 17.7$ and 22.9 T, respectively, which agrees well with the predicted value of ~22 T (linear interpolation between 120 and 150 GPa, Supplemental Material Table S3). The experimentally obtained H_{c2} and the isotope coefficient $\alpha = 0.49$ discussed below is in agreement with phonon-mediated superconductivity.

To determine the crystal structure, we analyzed the synchrotron x-ray diffraction (XRD) patterns [47–51]

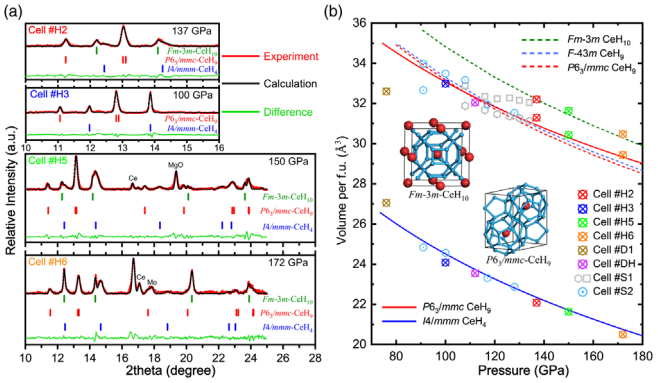

FIG. 2. XRD and P-V data of the Ce—H phases at different pressures. (a) Typical XRD (0.6199 Å) of the electrical cells H2, H3, H5, and H6. Relative phase fraction among CeH_{10}, CeH_9, and CeH_4 were estimated and presented in Fig. S3 [47,52]. (b) Pressure dependence of the cell volume per formula unit. Experimental data in this study are represented by different point symbols. Dashed and solid lines indicate the calculated P-V data and fitted experimental data from Ref. [36], respectively. More data are plotted in Fig. S2.

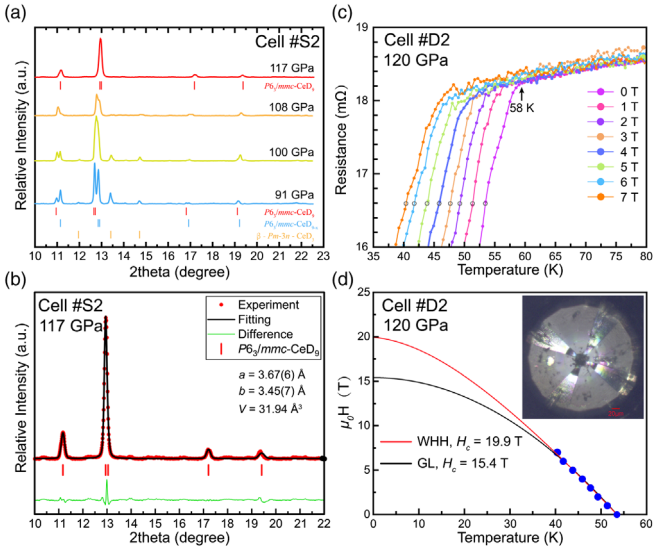

FIG. 3. XRD and electrical measurements in the external magnetic field of the synthesized Ce—D phases. (a) Selected XRD ($\lambda = 0.6199$ Å) of cell S2. (b) Le Bail refinement of cell S2 at 117 GPa (c) R-T dependence of the cell D2 in the external magnetic field of 0–7 T at 120 GPa. Circles represent the selected data for extrapolating $H_{c2}(0)$. (d) Upper critical magnetic field was extrapolated using the WHH [67] and GL [68,69] models. Inset is the photo of sample chamber.

and compared the experimentally obtained cell volumes with theoretical results (Fig. 2). Besides $P6_3/mmc$-CeH_9, two cubic phases $F\bar{4}3m$-CeH_9 [37,39] and $Fm\bar{3}m$-CeH_{10} [37–39,70] were predicted to be stable above 90 and 170 GPa, respectively, while they have not been reported in experiment. In this study, XRD reveals the existence of $I4/mmm$-CeH_4 and $P6_3/mmc$-CeH_9 in the cells H1–H6. At 172 GPa, the highest pressure we studied, a set of diffraction peaks from a cubic phase strikingly appeared in cell H6. Judging from the hydrogen content (or unit cell volume), we confirmed the presence of a new cubic phase $Fm\bar{3}m$-CeH_{10}. The appearance of this phase at much lower pressures than predicted could be due to H atoms' quantum motion in the anharmonic potential [28]. Besides, the delocalized nature of f electrons may also contribute to the lower stable pressure of CeH_{10} [71]. The lattice parameters and unit cell volumes of these phases are shown in Supplemental Material Table S2. Now, we can explain the steplike SC transitions with the presence of two high-temperature superconducting phases, $P6_3/mmc$-CeH_9 and $Fm\bar{3}m$-CeH_{10}.

According to Bardeen-Cooper-Schrieffer theory, conventional superconductors should exhibit the isotope effect. Considering that isotope substitution may influence the stability of Ce—H compounds, as reported in LaH_{10} [18], we performed structural investigation of the Ce—D system in three cells S1–S3 first. In the cell S1, $Fm\bar{3}m$-CeD_3 was synthesized at 12 GPa right after loading D_2. When pressure was further increased to 58 GPa, $I4/mmm$-CeD_4 formed. In contrast to the formation of $P6_3/mmc$-CeH_9 at around 100 GPa, CeD_4 remained stable up to 140 GPa though surrounded with a sufficient amount of deuterium (Fig. S26). After laser heating, we synthesized both $P6_3/mmc$-CeD_9 and $Fm\bar{3}m$-CeD_{10} (Fig. S27). As shown in Fig. 2(b) and Supplemental Material, Fig. S2, reducing the pressure of cell S1 leads to a series of successive transformations: at 116 GPa $Fm\bar{3}m$-CeD_{10} lost one deuterium and transformed into $Fm\bar{3}m$-CeD_9 that finally decomposed at about 90 GPa (gray squares). Simultaneously, the hydrogen desorption continues below 100 GPa (gray hexagons).

In cells S2 and S3, Ce was sandwiched in the fully deuterated ammonia borane (d-AB) [47,53]. Laser heating of the cell S2 at 91 GPa produced a mixture of β-$Pm\bar{3}n$-CeD_3, $I4/mmm$-CeD_4 and the target compound $P6_3/mmc$-CeD_9. The evolution of the selected XRD at different pressures is shown in Fig. 3(a). Two sets of diffraction signals are probably related to the hexagonal deuterides close to CeD_9. The same behavior was observed in hcp-I and hcp-II modifications of LaH_{10} [72]. Thus, we verified that $P6_3/mmc$-CeD_9 could be synthesized from Ce and d-AB with laser heating.

The change in T_c resulting from the substitution of hydrogen with deuterium provides direct evidence of the superconducting pairing mechanism, and we studied the isotope effect in the electrical cells D1–D3. In cell D1, $T_c = 25$ K was detected at 76 GPa, and the XRD revealed a mixture of β-$Pm\bar{3}n$-CeD_3 and $P6_3mc$-CeD_8 (Fig. S31). Cell D3 shows a peculiarity from the R-T curve at around 40 K and 100 GPa (Fig. S33). In cell D2, the onset of the superconducting transition was observed at 35 K (100 GPa,

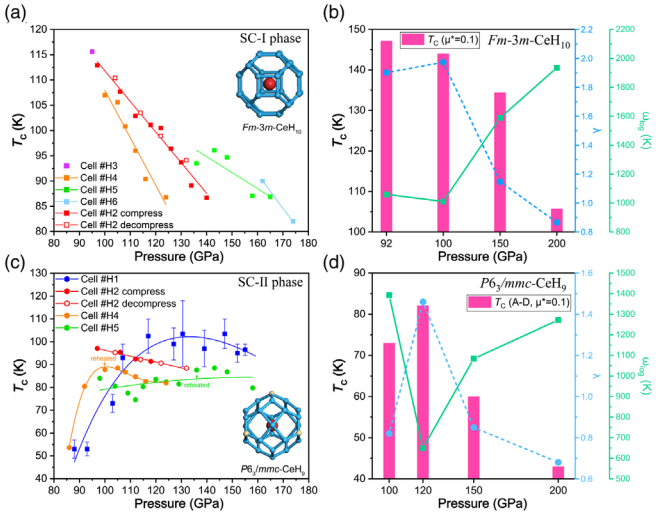

FIG. 4. Superconducting parameters of $Fm\bar{3}m$-CeH_{10} and $P6_3/mmc$-CeH_9. (a),(c) Experimental T_c as a function of pressure for phases SC-I and SC-II. Insets show the hydrogen cages, and yellow atoms represents the lost hydrogen from $P6_3/mmc$-CeH_9 to $P6_3mc$-CeH_8. (b),(d) Calculated logarithmic averaged frequency $\omega_{\log}$, EPC coefficient λ and T_c at various pressures for $Fm\bar{3}m$-CeH_{10} and $P6_3/mmc$-CeH_9. The theoretical data of $Fm\bar{3}m$-CeH_{10} are from Ref. [39].

Fig. S32) and 58 K [120 GPa, Fig. 3(c)]. The upper critical magnetic field estimated using the WHH and GL models reaches 19.9 and 15.4 T, respectively [Fig. 3(d)], which is in close agreement with the calculated value (~17 T at 120 GPa). We determined the isotope coefficient α using equation: $T_c(CeD_x) = T_c(CeH_x) \times m^{-\alpha}$, where m is the D/H mass ratio. Based on $T_{c1} \approx 82$ K in cell H4 or H5 and $T_{c2} \approx 58$ K in cell D2, the estimated isotope coefficient is equal to 0.49 for $P6_3/mmc$-CeH_9 at 120 GPa, close to theoretically predicted values (Supplemental Material, Table S3).

The earliest predicted T_c of $P6_3/mmc$-CeH_9 reaches 56 K at 100 GPa [38]. Salke *et al.* predicted the $T_c = 105 - 117$ K at 200 GPa, while mentioning that this phase should be unstable at pressures below 120 GPa and will distort to monoclinic $C2/c$-CeH_9 with $T_c = 63 - 75$ K at 100 GPa [37]. Simultaneously, $P6_3mc$-CeH_8 was predicted to be stable at 55–95 GPa. For $Fm\bar{3}m$-CeH_{10}, another work predicted maximum $T_c = 168$ K at 94 GPa [39]. Thus, one can expect that below 100 GPa, $Fm\bar{3}m$-CeH_{10} will have a higher T_c than $P6_3/mmc$-CeH_9. Figures 4(a) and 4(c) summarize the experimental pressure dependences of T_c of $Fm\bar{3}m$-CeH_{10} (SC-I) and $P6_3/mmc$-CeH_9 (SC-II). For phase SC-I, T_c reaches the maximum of 115 K at the lowest pressure (95 GPa), then decreases linearly as pressure increases. The decompression $T_c - P$ data for the sample in cell H2 further confirmed this dependence. Phase SC-II shows a different trend, displaying a domelike $T_c(P)$ dependence [Fig. 4(c)] observed earlier in H_3S [73] and LaH_{10} [18,72].

Superconductivity is very sensitive to stoichiometry and structural distortions. The deviation from the ideal stoichiometric Ce: H ratio and various degree of distortion are the main causes of inconsistent results obtained from different cells. We have previously observed a continuous increase of cell volume during compression from 80 to 103 GPa without laser heating [36], representing the gradual increase of hydrogen stoichiometry to the ideal ratio 1:9. In contrast, Salke *et al.* [37] reported the direct formation of CeH_9 after heating to over 1700 K at 80 GPa. This indicates the competition between $P6_3mc$-CeH_8 and $C2/c$-CeH_9, depending on the heating temperature. In another aspect, we cannot ensure the released H_2 from AB is sufficient in each cell. The possible non-stoichiometry will also affect the degree of distortion of $C2/c$-CeH_9, while it is indistinguishable in x-ray diffraction (the same situation as in H_3S [73] and LaH_{10} [72]).

As shown in Fig. 4d and Supplemental Material, Table S3, results of *ab initio* calculations for $P6_3/mmc$-CeH_9 are in agreement with the observed experimental trends [47,54–65,74–77]. In the pressure range from 100 to 120 GPa, the EPC coefficient λ increases from 0.82 to 1.46, and T_c rises from 73 K and reaches a maximum of 82 K ($\mu^* = 0.1$) in qualitative agreement with our experimental results. Simultaneously, the density of electron states at the Fermi level $N(E_F) = 0.92$ states/eV/Ce and the upper critical magnetic field $[\mu_0 H_C(0) \sim 17$ T] also reach maximum values probably due to the $C2/c \rightarrow P6_3/mmc$ phase transition. For pressures above 120 GPa, stabilization of $P6_3/mmc$-CeH_9 leads to an increase in the logarithmic frequency $\omega_{\log}$ and the Debye temperature with a simultaneous decrease in the EPC coefficient and the critical temperature of superconductivity. The same situation occurs for $Fm\bar{3}m$-CeH_{10} in the pressure range of 100–200 GPa [Fig. 4(b)], as λ drops from 2.0 to 0.8 and T_c decreases monotonically, in close agreement with the experimental tendency [Fig. 4(a)]. In contrast with the experimentally obtained lower T_c of cubic LaH_{10}, and YH_6, our experimentally obtained $P6_3/mmc$-CeH_9 at pressures above 120 GPa shows a 10–20 K higher T_c than the predicted one [47,78–83]. Anisotropy of the superconducting gap is one of possible reasons for the unusual underestimation of T_c by theory. The partial electron-phonon coupling coefficients vary among different q points (Table S5), and the estimated T_c increased to 104 K considering only $q1$ and $q7$ within the optimized tetrahedron method (Fig. S37). This can be verified in the future and requires a better crystallized sample.

Conclusions.—Synthesis and comprehensive study of superconductivity of superhydrides and superdeutrides ($Fm\bar{3}m$-CeH_{10},$P6_3/mmc$-CeH_9, $Fm\bar{3}m$-CeD_{10}, $F\bar{4}3m$-CeD_9, $P6_3/mmc$-CeD_9, $P6_3mc$-CeD_8, $P6_3mc$-CeD_6, and $I4/mmm$-CeD_4) showed that cerium hydrides are remarkable compounds. Stable and displaying

high-temperature superconductivity at lower pressures than any other superhydrides, they serve as an ideal starting point to further study the mechanism of superconductivity in these fascinating compounds, and design other superconductors, stable at even lower pressures. Soft-mode-driven phase transition in CeH_9 is responsible for a maximum in T_c, and this can be used for engineering higher-temperature superconductors. Away from the phase transition, T_c of both CeH_9 and CeH_{10} decreases with pressure, leading one to hope that search for superconductors with lower-pressure stability can lead to increased T_c.

In situ angle dispersive XRD were performed at 4W2 HP-Station, Beijing Synchrotron Radiation Facility (BSRF), and 15U1 beamline, Shanghai Synchrotron Radiation Facility (SSRF). This work was supported by the National Key R&D Program of China (No. 2018YFA0305900), National Natural Science Foundation of China (No. 51572108, No. 11974133, No. 51720105007), and Program for Changjiang Scholars, Innovative Research Team in University (No. IRT_15R23). D. V. S. was funded by the Russian Foundation for Basic Research (Project No. 20-32-90099). A. R. O is supported by the Ministry of Science and Higher Education (Grant No. 2711.2020.2 to leading scientific schools). We thank Yonghao Han (Jilin University) for the instructions on preparing Mo electrodes and Igor Grishin (Skoltech) for proofreading of the manuscript.

*Corresponding author.
huangxiaoli@jlu.edu.cn
†Corresponding author.
cuitian@nbu.edu.cn

[1] H. K. Onnes, Proc. K. Ned. Akad. Wet. **13**, 1274 (1911), http://scholar.google.com/scholar?hl=en&q=H.+K.+Onnes%2C+Proc.+K.+Ned.+Akad.+Wet.+13%2C+1274+%281911%29.
[2] J. Nagamatsu, N. Nakagawa, T. Muranaka, Y. Zenitani, and J. Akimitsu, Nature (London) **410**, 63 (2001).
[3] J. G. Bednorz and K. A. Müller, Z. Phys. B **64**, 189 (1986).
[4] E. Wigner and H. B. Huntington, J. Chem. Phys. **3**, 764 (1935).
[5] J. M. McMahon, M. A. Morales, C. Pierleoni, and D. M. Ceperley, Rev. Mod. Phys. **84**, 1607 (2012).
[6] S. Azadi, B. Monserrat, W. M. C. Foulkes, and R. J. Needs, Phys. Rev. Lett. **112**, 165501 (2014).
[7] J. McMinis, R. C. Clay, D. Lee, and M. A. Morales, Phys. Rev. Lett. **114**, 105305 (2015).
[8] N. W. Ashcroft, Phys. Rev. Lett. **21**, 1748 (1968).
[9] P. Cudazzo, G. Profeta, A. Sanna, A. Floris, A. Continenza, S. Massidda, and E. K. U. Gross, Phys. Rev. Lett. **100**, 257001 (2008).
[10] B. Monserrat, N. D. Drummond, P. Dalladay-Simpson, R. T. Howie, P. López Ríos, E. Gregoryanz, C. J. Pickard, and R. J. Needs, Phys. Rev. Lett. **120**, 255701 (2018).
[11] C. J. Pickard, I. Errea, and M. I. Eremets, Annu. Rev. Condens. Matter Phys. **11**, 57 (2020).
[12] D. V. Semenok, I. A. Kruglov, and A. G. Kvashnin, Curr. Opin. Solid State Mater. Sci. **24**, 100808 (2020).
[13] D. Duan, Y. Liu, Y. Ma, Z. Shao, B. Liu, and T. Cui, Natl. Sci. Rev. **4**, 121 (2016).
[14] M. J. Hutcheon, A. M. Shipley, and R. J. Needs, Phys. Rev. B **101**, 144505 (2020).
[15] E. Zurek and T. Bi, J. Chem. Phys. **150**, 050901 (2019).
[16] J. A. Flores-Livas, L. Boeri, A. Sanna, G. Profeta, R. Arita, and M. Eremets, Phys. Rep. **856**, 1 (2020).
[17] N. W. Ashcroft, Phys. Rev. Lett. **92**, 187002 (2004).
[18] A. P. Drozdov, P. P. Kong, V. S. Minkov, S. P. Besedin, M. A. Kuzovnikov, S. Mozaffari, L. Balicas, F. F. Balakirev, D. E. Graf, V. B. Prakapenka, E. Greenberg, D. A. Knyazev, M. Tkacz, and M. I. Eremets, Nature (London) **569**, 528 (2019).
[19] M. Somayazulu, M. Ahart, A. K. Mishra, Z. M. Geballe, M. Baldini, Y. Meng, V. V. Struzhkin, and R. J. Hemley, Phys. Rev. Lett. **122**, 027001 (2019).
[20] D. V. Semenok, A. G. Kvashnin, A. G. Ivanova, V. Svitlyk, V. Y. Fominski, A. V. Sadakov, O. A. Sobolevskiy, V. M. Pudalov, I. A. Troyan, and A. R. Oganov, Mater. Today **33**, 36 (2020).
[21] A. P. Drozdov, M. I. Eremets, I. A. Troyan, V. Ksenofontov, and S. I. Shylin, Nature (London) **525**, 73 (2015).
[22] I. A. Troyan, D. V. Semenok, A. G. Kvashnin, A. V. Sadakov, O. A. Sobolevskiy, V. M. Pudalov, A. G. Ivanova, V. B. Prakapenka, E. Greenberg, A. G. Gavriliuk, I. S. Lyubutin, V. V. Struzhkin, A. Bergara, I. Errea, R. Bianco, M. Calandra, F. Mauri, L. Monacelli, R. Akashi, and A. R. Oganov, Adv. Mater. **33**, 2006832 (2021).
[23] P. P. Kong, V. S. Minkov, M. A. Kuzovnikov, S. P. Besedin, A. P. Drozdov, S. Mozaffari, L. Balicas, F. F. Balakirev, V. B. Prakapenka, E. Greenberg, D. A. Knyazev, and M. I. Eremets, arXiv:1909.10482.
[24] A. P. Drozdov, M. I. Eremets, and I. A. Troyan, arXiv:1508.06224.
[25] D. F. Duan, Y. X. Liu, F. B. Tian, D. Li, X. L. Huang, Z. L. Zhao, H. Y. Yu, B. B. Liu, W. J. Tian, and T. Cui, Sci. Rep. **4**, 6968 (2014).
[26] X. L. Huang, X. Wang, D. F. Duan, B. Sundqvist, X. Li, Y. P. Huang, H. Y. Yu, F. F. Li, Q. Zhou, B. B. Liu, and T. Cui, Natl. Sci. Rev. **6**, 713 (2019).
[27] H. Y. Liu, I. I. Naumov, R. Hoffmann, N. W. Ashcroft, and R. J. Hemley, Proc. Natl. Acad. Sci. U.S.A. **114**, 6990 (2017).
[28] I. Errea, F. Belli, L. Monacelli, A. Sanna, T. Koretsune, T. Tadano, R. Bianco, M. Calandra, R. Arita, F. Mauri, and J. A. Flores-Livas, Nature (London) **578**, 66 (2020).
[29] E. Snider, N. Dasenbrock-Gammon, R. McBride, M. Debessai, H. Vindana, K. Vencatasamy, K. V. Lawler, A. Salamat, and R. P. Dias, Nature (London) **586**, 373 (2020).
[30] E. Snider, N. Dasenbrock-Gammon, R. McBride, X. Wang, N. Meyers, K. V. Lawler, E. Zurek, A. Salamat, and R. P. Dias, Phys. Rev. Lett. **126**, 117003 (2021).
[31] Y. Sun, J. Lv, Y. Xie, H. Liu, and Y. Ma, Phys. Rev. Lett. **123**, 097001 (2019).
[32] S. Di Cataldo, C. Heil, W. Von Der Linden, and L. Boeri, Phys. Rev. B **104**, L020511 (2021).
[33] R. J. Hemley, M. Ahart, H. Liu, and M. Somayazulu, arXiv:2012.13398.

[34] Z. Zhang and T. Cui, M. J. Hutcheon, A. M. Shipley, H. Song, M. Du, V. Z. Kresin, D. Duan, C. J. Packard, and Y. Yao,arXiv:2106.09879v2.

[35] X. Liang, A. Bergara, X. Wei, L. Wang, R. Sun, H. Liu, Russell, L. Wang, G. Gao, and Y. Tian, arXiv:2107.02553.

[36] X. Li, X. L. Huang, D. F. Duan, C. J. Pickard, D. Zhou, H. Xie, Q. Zhuang, Y. P. Huang, Q. Zhou, B. B. Liu, and T. Cui, Nat. Commun. **10**, 3461 (2019).

[37] N. P. Salke, M. M. Davari Esfahani, Y. Zhang, I. A. Kruglov, J. Zhou, Y. Wang, E. Greenberg, V. B. Prakapenka, J. Liu, A. R. Oganov, and J.-F. Lin, Nat. Commun. **10**, 4453 (2019).

[38] F. Peng, Y. Sun, C. J. Pickard, R. J. Needs, Q. Wu, and Y. M. Ma, Phys. Rev. Lett. **119**, 107001 (2017).

[39] B. Li, Z. Miao, L. Ti, S. Liu, J. Chen, Z. Shi, and E. Gregoryanz, J. Appl. Phys. **126**, 235901 (2019).

[40] Y. V. Kondrat'ev, A. V. Butlak, I. V. Kazakov, and A. Y. Timoshkin, Thermochim. Acta **622**, 64 (2015).

[41] Y. Sun, J. Chen, V. Drozd, S. Najiba, and C. Bollinger, J. Phys. Chem. Solids **84**, 75 (2015).

[42] J. Nylén, T. Sato, E. Soignard, J. L. Yarger, E. Stoyanov, and U. Häussermann, J. Chem. Phys. **131**, 104506 (2009).

[43] D. Zhou, D. V. Semenok, H. Xie, X. L. Huang, D. F. Duan, A. Aperis, P. M. Oppeneer, M. Galasso, A. I. Kartsev, A. G. Kvashnin, A. R. Oganov, and T. Cui, J. Am. Chem. Soc. **142**, 2803 (2020).

[44] D. Zhou, D. V. Semenok, D. Duan, H. Xie, W. Chen, X. Huang, X. Li, B. Liu, A. R. Oganov, and T. Cui, Sci. Adv. **6**, eaax6849 (2020).

[45] B. J. Baer, M. E. Chang, and W. J. Evans, J. Appl. Phys. **104**, 034504 (2008).

[46] Y. Akahama and H. Kawamura, J. Appl. Phys. **100**, 043516 (2006).

[47] See Supplemental Material at http://link.aps.org/supplemental/10.1103/PhysRevLett.127.117001 for synchrotron x-ray diffraction measurements, for additional data for the experimental diamond anvil cells, for sample preparation and electrical resistance measurements, for theoretical calculations, and for *ab initio* calculations of superconducting parameters of CeH_9 at 120–200 GPa, which includes Refs. [48–65].

[48] A. Le Bail, H. Duroy, and J. L. Fourquet, Mater. Res. Bull. **23**, 447 (1988).

[49] R. A. Young, Int. Union Cryst. **30**, 494 (1995).

[50] V. Petříček, M. Dušek, and L. Palatinus, Z. Kristallogr. Cryst. Mater. **229**, 345 (2014).

[51] C. Prescher and V. B. Prakapenka, High Press. Res. **35**, 223 (2015).

[52] B. H. Toby and R. B. Von Dreele, J. Appl. Crystallogr. **46**, 544 (2013).

[53] V. M. Parvanov, G. K. Schenter, N. J. Hess, L. L. Daemen, M. Hartl, A. C. Stowe, D. M. Camaioni, and T. Autrey, Dalton Trans. 4514 (2008).

[54] P. Giannozzi *et al.*, J. Phys. Condens. Matter **21**, 395502 (2009).

[55] P. Giannozzi *et al.*, J. Phys. Condens. Matter **29**, 465901 (2017).

[56] R. Hill, Proc. Phys. Soc. London Sect. A **65**, 349 (1952).

[57] J. M. Ziman, *Electrons and Phonons* (Clarendon Press, Oxford, 1960).

[58] O. L. Anderson, J. Phys. Chem. Solids **24**, 909 (1963).

[59] G. Bergmann and D. Rainer, Z. Phys. **263**, 59 (1973).

[60] P. B. Allen and R. C. Dynes, Technical Report No. 7 TCM41974, 1974.

[61] P. B. Allen and R. C. Dynes, Phys. Rev. B **12**, 905 (1975).

[62] J. P. Carbotte, Rev. Mod. Phys. **62**, 1027 (1990).

[63] S. Goedecker, M. Teter, and J. Hutter, Phys. Rev. B **54**, 1703 (1996).

[64] C. Hartwigsen, S. Goedecker, and J. Hutter, Phys. Rev. B **58**, 3641 (1998).

[65] P. Ravindran, L. Fast, P. A. Korzhavyi, B. Johansson, J. Wills, and O. Eriksson, J. Appl. Phys. **84**, 4891 (1998).

[66] C. Gao, Y. Han, Y. Ma, A. White, H. Liu, J. Luo, M. Li, C. He, A. Hao, X. Huang, Y. Pan, and G. Zou, Rev. Sci. Instrum. **76**, 083912 (2005).

[67] N. R. Werthamer, E. Helfand, and P. C. Hohenberg, Phys. Rev. **147**, 295 (1966).

[68] V. L. Ginzburg and L. D. Landau, Zh. Eksp. Teor. Fiz. **20**, 1064 (1950).

[69] J. A. Woollam, R. B. Somoano, and P. O'Connor, Phys. Rev. Lett. **32**, 712 (1974).

[70] P. Tsuppayakorn-aek, U. Pinsook, W. Luo, R. Ahuja, and T. Bovornratanaraks, Mater. Res. Express **7**, 086001 (2020).

[71] H. Jeon, C. Wang, S. Yi, and J.-H. Cho, Sci. Rep. **10**, 16878 (2020).

[72] D. Sun, V. S. Minkov, S. Mozaffari, S. Chariton, V. B. Prakapenka, M. I. Eremets, L. Balicas, and F. F. Balakirev, arXiv:2010.00160.

[73] M. Einaga, M. Sakata, T. Ishikawa, K. Shimizu, M. I. Eremets, A. P. Drozdov, I. A. Troyan, N. Hirao, and Y. Ohishi, Nat. Phys. **12**, 835 (2016).

[74] S. Baroni, S. de Gironcoli, A. Dal Corso, and P. Giannozzi, Rev. Mod. Phys. **73**, 515 (2001).

[75] M. l. Wierzbowska, S. d. Gironcoli, and P. Giannozzi, arXiv:cond-mat/0504077.

[76] M. Kawamura, Y. Gohda, and S. Tsuneyuki, Phys. Rev. B **89**, 094515 (2014).

[77] E. F. Talantsev, arXiv:2004.03155.

[78] D. Gajda, A. Morawski, A. J. Zaleski, W. Häßler, K. Nenkov, M. A. Rindfleisch, E. Żuchowska, G. Gajda, T. Czujko, T. Cetner, and M. S. A. Hossain, J. Appl. Phys. **117**, 173908 (2015).

[79] A. Sanna, G. Profeta, A. Floris, A. Marini, E. K. U. Gross, and S. Massidda, Phys. Rev. B **75**, 020511 (2007).

[80] T.-R. Yang, S. Patapis, O. Furdui, V. Toma, A. V. Pop, and G. Ilonca, Int. J. Mod. Phys. B **17**, 2845 (2003).

[81] G. M. Eliashberg, J. Exp. Theor. Phys. **11**, 696 (1959).

[82] L. Landau, Phys. Rev. **60**, 356 (1941).

[83] J. P. Perdew, K. Burke, and M. Ernzerhof, Phys. Rev. Lett. **77**, 3865 (1996).